Electrochemistry Communications 116 (2020) 106763

Contents lists available at ScienceDirect

Electrochemistry Communications

journal homepage: www.elsevier.com/locate/elecom

Design of an electrochemically gated organic semiconductor for pH sensing

Federica Mariani[a], Isacco Gualandi[a], Domenica Tonelli[a], Francesco Decataldo[b], Luca Possanzini[b], Beatrice Fraboni[b], Erika Scavetta[a,*]

[a] Dipartimento di Chimica Industriale "Toso Montanari", Università di Bologna, Viale del Risorgimento 4, 40136 Bologna, Italy
[b] Dipartimento di Fisica e Astronomia, Università di Bologna, Viale Berti Pichat 6/2, 40127 Bologna, Italy

ARTICLE INFO

Keywords:
pH detection
Electrochemical sensor
Wearable sensor
Electrochemical gating
PEDOT:PSS
PEDOT:BTB

ABSTRACT

Since the development of potentiometric ion-selective electrodes, remarkable steps have been taken towards progressive simplification and improved robustness of pH sensing probes. In particular, the design of compact sensing architectures using solid-state components holds great potential for portable and wearable applications. Here we report the development of an electrochemically gated device for pH detection, combining the robustness of potentiometric-like transduction with an extremely simple and integrated geometry requiring no reference. The sensor is a two-point probe device comprising two thin polymeric films, i.e. a charge transport layer and a pH-sensitive layer, and exhibits a sensitivity of $(8.3 \pm 0.2) \times 10^{-3}$ pH unit^{-1} in the pH range from 2 to 7. Thanks to the versatility and robustness of the optimised design, a textile pH sensor was fabricated whose performance is comparable with that of glass sensors.

1. Introduction

pH regulation is essential to sustain life and the detection of changes in pH can provide diagnostic information about health and body status. A cascade of compensatory mechanisms crossing organ-specific boundaries competes in maintaining the acid-base homeostasis in the human body [1] and include buffering systems of both intra- and extracellular fluids, as well as respiratory and renal control of the plasma pH [2]. Dysregulation of pH in different fluid compartments and its impact on physiological functions are of interest in both routine clinical analysis and biomedical research. A novel frontier in healthcare applications is represented by the analysis of biofluids that can be conveniently collected in a non-invasive manner, thus allowing continuous and real-time on-body monitoring of biologically relevant markers. In particular, pH variations in human sweat have been correlated to blood glucose levels [3], the presence of genetic disorders such as cystic fibrosis [4,5] and metabolic alkalosis during sports activity [6,7], while the pH of a wound exudate is indicative of the progression of the wound-healing process and the presence of bacterial colonies [8,9]. Real-time analysis of such biofluids can be achieved by means of portable and wearable sensing devices integrated into clothing, bandages or everyday accessories. In addition to wear-and-forget functionality, ease of use, robustness, low power consumption and simple readout electronics are mandatory requirements of wearable devices and these pose several challenges to conventional chemical sensors [10,11].

Quantitative pH analysis is dominated by electrochemical methods, whose use and development span more than a century [12]. The glass electrode has long held primacy in pH measurement thanks to its excellent performance in terms of sensitivity, long-term stability, selectivity and inactivity vs redox systems [13] and it is in daily use in research laboratories and industry. However, the electrode components ensuring the aforementioned performance i.e. the proton-exchange glass membrane and the internal liquid reference system, also represent major drawbacks to the system, such as mechanical fragility, difficulty in miniaturization and potential contamination of tested samples, thus hindering the use of the glass pH electrode in biotechnology applications [14], the food industry [15], environmental analysis [16] and portable electronics [17]. Nonetheless, there has been extensive materials and technology research aimed at a progressive simplification and improved robustness of the sensing probes. The development of all-solid-state glass and glass-less pH electrodes has significantly reduced the limitations related to storage and miniaturisation of potentiometric probes [13,16,18,19]. Along with the indicator, miniaturisation of the reference electrode (RE) remains a major challenge. While simple miniaturisation of a bulk RE results in a short lifetime and unstable junction potential [20], elimination of the reference solution compartment has been pursued in the design of solid-state and screen-printed REs and pseudo-REs. In such cases, while potential drift and sensitivity to anions limit the application of pseudo-REs to laboratory use, the development of reliable screen-printed REs is still only at a

* Corresponding author.
E-mail address: erika.scavetta2@unibo.it (E. Scavetta).

https://doi.org/10.1016/j.elecom.2020.106763
Received 5 May 2020; Received in revised form 19 May 2020; Accepted 28 May 2020
Available online 31 May 2020

basic level and the performance of the bulk counterpart remains unmatched [21,22]. Among miniaturised solid-state devices for pH sensing, ion-sensitive field effect transistors (ISFETs) have benefited from seamless integration with electronic manufacturing processes, such as complementary metal-oxide semiconductors (CMOS), which provide rapid development to commercialisation. First introduced by P. Bergeveld in 1970 [23], ISFETs pH sensors have a traditional FET structure where the metal gate electrode is removed and the gate dielectric is exposed to the analyte solution. At this interface, a pH-dependent surface charge alters the electric field and modulates the conductivity of the channel [20]. With improved robustness, faster response time and potential to combine sensing and amplification elements on-chip, ISFETs have found commercial use [24–26] in those market segments where the vulnerability of glass electrodes hindered pH detection [27]. However, sub-Nernstian response and the inescapable need for a large reference electrode still limits the appeal of such miniaturized indicator devices [17].

In this scenario, the use of organic electrochemical transistors (OECTs) to fabricate referenceless sensors with potentiometric transduction has been recently reported by our group [28]. Still based on the transistor architecture, dual-gate FETs with a Parylene C pH sensing layer [29] and a thioamine-functionalised gate electrode [30], an iridium oxide-modified OECT for differential pH measurement [31] and an all-polymeric OECT based on the conducting polymer poly(3,4-ethylenedioxythiophene) (PEDOT) doped with a pH sensitive dye [32] have been fabricated, leading to highly integrated pH sensors based on flexible substrates and showing super-Nernstian sensitivities. With the aim of further simplification of the referenceless, three-terminal transistor architecture, innovative gateless configurations have been recently proposed [33]. In particular, the concept of chemically driven electrostatic gating was introduced to obtain a two-terminal, FET sensor for DNA, comprising a semiconducting charge transport element, i.e. a single-walled carbon nanotube (SWCNT), nested in a charged functional shell. Here, binding of the analyte at surface receptor groups led to electrostatic modulation of the conductivity in the SWCNT, in analogy with the effect of a gate voltage in a chemically sensitive FET [34]. Similarly, our group reported a two-terminal sensor for Cl^- detection, in which Ag/AgCl NPs were embedded within a PEDOT-based film. Thanks to the Nernstian redox activity of the NPs in the presence of chloride anions in the sample solution, a spontaneous electrochemical gating modulates the polymer conductivity with no need for a free-standing gate electrode, thus allowing a two-terminal Cl^- sensor to be achieved on a cotton thread [35]. Here we report the design of an electrochemically gated pH sensor with a simple, two-terminal configuration, comprising a charge transport layer made of PEDOT doped with poly(styrenesulfonate) (PSS) and a pH-sensitive layer. The latter is based on the Nernstian transducer PEDOT:Bromothymol Blue (PEDOT:BTB) [36], whose use as the gate material in an OECT sensor for pH detection was recently reported by our group [32]. Firstly, we characterise the transduction mechanism originating the sensitivity to pH variations in PEDOT:BTB and we demonstrate that it relies on spontaneous redox events, which is an essential feature for the chemically-sensitive layer of an electrochemically gated device. Then, we show the operation of the two-terminal device, in which the conductivity of the charge transport layer is modulated in a pH-dependent fashion upon contact with the PEDOT:BTB film, without the need for a physically separated pH-sensitive gate electrode. We assess and exploit the major advantage of the two-terminal pH sensor, i.e. its simple and versatile geometry, by fabricating a textile-based pH sensor for wearable applications.

2. Experimental

2.1. Chemicals and buffers

CLEVIOS™ pH 1000 suspension (PEDOT:PSS) was purchased from Heraeus. 3,4-ethylenedioxythiophene (EDOT), bromothymol blue (BTB), (3-glycidyloxypropyl)trimethoxysilane (GOPS), sodium dodecylbenzenesulfonate, potassium nitrate, potassium hydroxide, nitric acid, acetic acid, 85% phosphoric acid and boric acid were purchased from Sigma Aldrich. Monobasic potassium phosphate was bought from Fluka. Ethylene glycol (EG) was obtained from Carlo Erba. Silicone elastomer and a curing agent for preparation of PDMS were obtained from Sylgard. All chemicals were of reagent grade or higher. The phosphate buffer solution (PBS) was made from 0.1 M KH_2PO_4 and corrected to pH 7.0 by addition of 1 M KOH. The universal buffer (U.B.) solution was made from 0.01 M H_3PO_4, 0.01 M H_3BO_3 and 0.01 M CH_3COOH in 0.1 M KNO_3.

2.2. Apparatus

All potential-controlled measurements were carried out in a single compartment, a three-electrode cell, using a potentiostat (CH Instrument 660C). Electrode potentials were measured with respect to an aqueous saturated calomel electrode (SCE) and a Pt wire was used as the counter electrode. A combined glass electrode (Amel 411/CGG/12) connected to a pH meter (Amel instruments 338) was employed for pH measurements. Morphology characterization and thickness evaluation of the polymeric films were carried out in air at room temperature using an atomic force microscopy (AFM) Park System NX10 in tapping mode.

2.3. Fabrication of sensors on a glass substrate

The device consists of two parallel Cr/Au electrodes with a polymeric film between them (0.4 × 0.8 cm^2), comprising a PEDOT:PSS layer deposited by spin-coating and a PEDOT:BTB layer formed by electrochemical deposition. The conductive materials were deposited on a glass slide using the following procedure. The Cr/Au (50 nm) strips were deposited via thermal evaporation using a mask. Then, PEDOT:PSS was deposited to partly overlap the two gold electrodes. A CLEVIOS™ pH 1000 suspension was mixed with ethylene glycol (secondary dopant), dodecylbenzene sulfonic acid (surfactant), and 3-glycidyloxypropyltrimethoxysilane (cross linker) in the following volumetric ratio: 78.95:20:0.05:1. The solution was sonicated for 10 min before spinning. The glass substrates were cleaned sequentially in sonicating baths of deionized water, acetone and isopropanol for 15 min. The substrates were then masked and the PEDOT:PSS solution was spun cast at 500 rpm. PEDOT:BTB was electrosynthesised by cyclic voltammetry, following a previously reported procedure [32]. Briefly, the polymerisation solution (PS) comprised 10 mM EDOT, 1 mM BTB and 1 mM PBS (pH 7.0) in 0.1 M KNO_3 aqueous solution. The PS was stirred for 15 min and then electrodeposition was carried out in a three-electrode cell, where the two gold terminals were shorted together and connected as the WE in the electrochemical cell. A potential ramp ranging from 0 to 1 V was applied to the WE with a scan rate of 0.1 V s^{-1} for 5 or 10 cycles. After electrodeposition, the blue iridescent film of PEDOT:BTB covering the PEDOT:PSS layer was rinsed with distilled water.

2.4. Fabrication of textile-based sensors

A conducting ink was made with 79% v/v PH1000, 20% v/v EG and 1% v/v GOPS. In order to obtain a suitable viscosity for deposition, the ink was warmed in an oven at 70 °C to lose about 40% of its initial weight. A mask was then employed to screen-print the desired pattern (2 × 0.5 cm^2 strips) onto a bio-ceramic fabric, which was then allowed to dry for 10 min at 40 °C. Afterwards, commercial conducting threads were sewn at the edges of the printed pattern and the knots were coated with Ag paste and insulated with PDMS, obtained by mixing silicone elastomer and curing agent in a 10:1 w/w ratio, and then cured by placing the textile devices on a hot plate at 140 °C for 10 min. PEDOT:BTB was then electrodeposited on the printed PEDOT:PSS layer

following the procedure described in section 2.3.

2.5. pH measurements in the two-terminal configuration

The two terminal sensors were connected to a Source-measure Unit (Keysight B2902A). One terminal was set to ground and a fixed potential of −200 mV was applied to the other, while the generated current was measured vs time. All tests were performed in U.B. and the solution pH was changed by dropwise addition of 1 M KOH or 1 M HNO_3 under gentle stirring. The exact pH value of the solution following each addition was determined in blank experiments using a glass electrode.

3. Results and discussion

3.1. Potentiometric vs. Amperometric response of PEDOT:BTB

PEDOT:BTB is a semiconducting material in which acid-base equilibria involving the dye counterion BTB promote the formation of pH-dependent electronic states in the conjugated polymer, thus originating pH sensitivity [32]. In order to achieve further understanding of the nature of the transduction mechanism, the potentiometric and amperometric responses of a PEDOT:BTB/GCE (glassy carbon electrode) were recorded and are compared in Fig. 1.

Both the electrochemical potential, E (Fig. 1A) and the current, I (Fig. 1B) were recorded vs. time while 1 M KOH was added in a stepwise manner to the Universal Buffer solution (U.B.). In the potentiometric experiment, E (i.e. the open circuit potential) represents the thermodynamic tendency of PEDOT:BTB to change its redox state upon interaction with the electrolyte. A decrease in E occurs as the electrolyte pH moves towards more alkaline values, suggesting that electron extraction becomes more and more favoured, in analogy with previous findings [32,36]. The electrochemical reaction that takes place at the electrode/electrolyte interface is the following:

$$2PEDOT^{+}: BTB^{2-} + e^{-} + H^{+} \rightleftarrows PEDOT + PEDOT^{+}: BTB^{-}$$

and, since it is a monoelectronic process, the variation in the electrochemical potential due to pH changes in standard conditions is described by the Nernst equation:

$$E = E^{0} + 0.05916\log\frac{[2PEDOT^{+}: BTB^{2-}][H^{+}]}{[PEDOT][PEDOT^{+}: BTB^{-}]}$$

where E^{0} is the standard reduction potential of the redox couple $PEDOT^{+}$/PEDOT. According to this, steady-state E values can be linearly correlated to variations in pH (Fig. 1A) in the pH interval 2–7, with a slope equal to 43 ± 1 mV pH $unit^{-1}$. By contrast, application of a fixed potential to the working electrode (set equal to the open circuit potential measured in U.B. at pH 2.2, E_{app} = 0.246 V vs SCE) hampers the spontaneous redox events that are responsible for the pH-dependent response (Fig. 1B) and no variation of the steady-state current is observed. Summarizing, PEDOT:BTB transduces a pH signal through the generation of an electromotive force at the solid/liquid interface, which can be measured with respect to a reference electrode.

3.2. Design of a two-terminal pH sensor based on PEDOT:BTB/PEDOT:PSS multilayer

The use of PEDOT:BTB as the gate material in an organic transistor was recently reported by our group [32]. This led to the development of a three-terminal pH sensor chip, where the pH-dependent modulation of the current flowing through a semiconducting channel made of PEDOT:PSS was achieved upon application of two small input voltages,

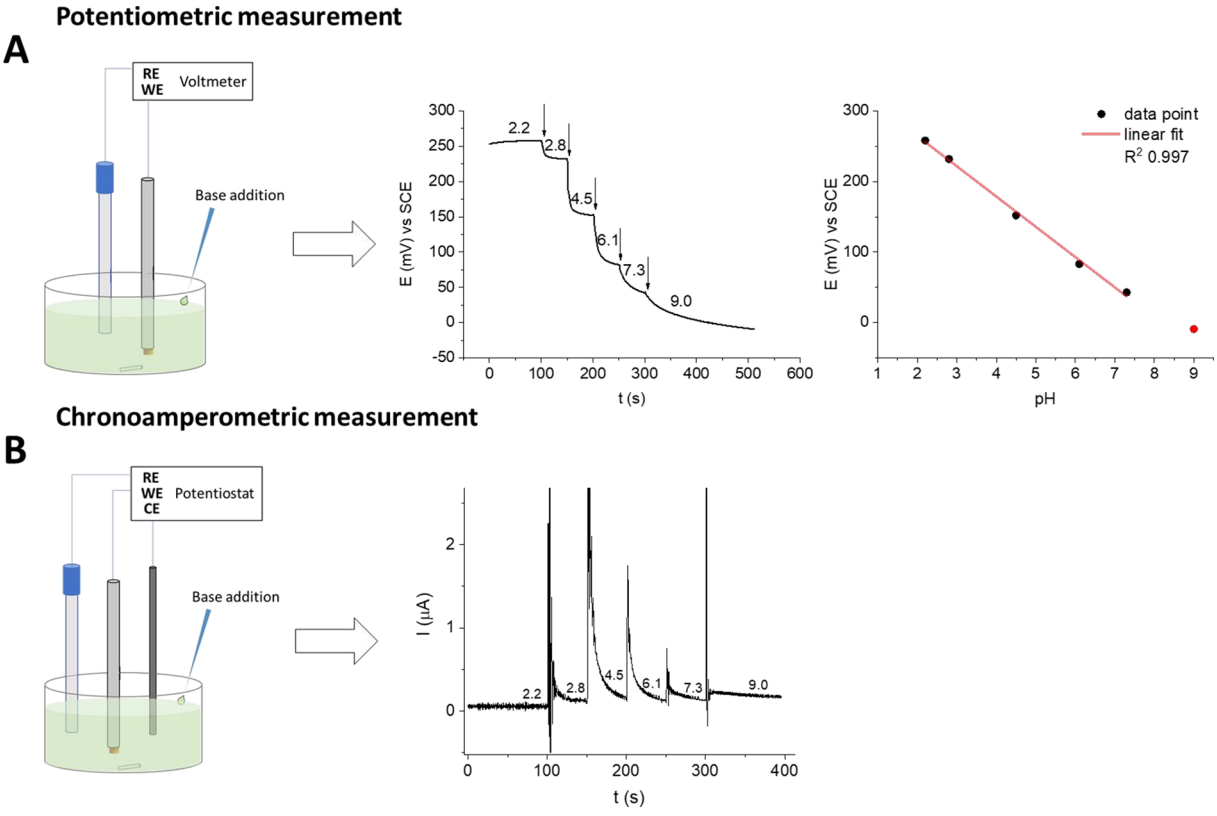

Fig. 1. Potentiometric vs. amperometric response of PEDOT:BTB. (A) Potentiometric experimental setup used to record the electrochemical potential vs time of PEDOT:BTB/GCE during addition of 1 M KOH to a Universal Buffer solution and calibration plot obtained from the potentiometric response (R^2 0.997). (B) Amperometric experimental setup used to record the current vs time response of PEDOT:BTB/GCE during addition of 1 M KOH to a Universal Buffer solution. E_{app} = 0.246 V vs SCE. The addition times are indicated by arrows and the numbers correspond to the pH of the solution.

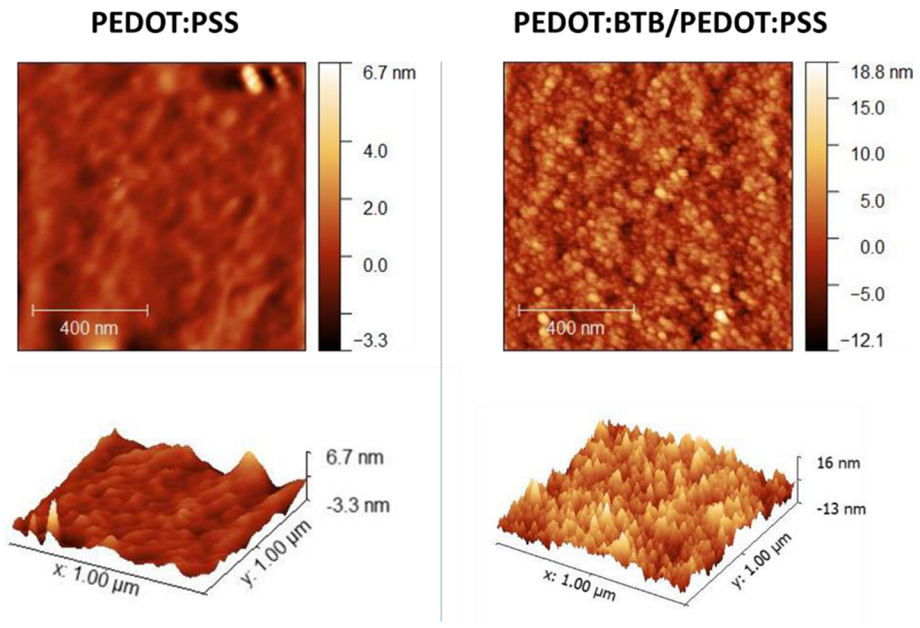

Fig. 2. Morphology characterisation. AFM images and 3D maps of the spin-coated PEDOT:PSS film (left) and the PEDOT:BTB/PEDOT:PSS film (right) obtained after 10 PEDOT:BTB deposition cycles.

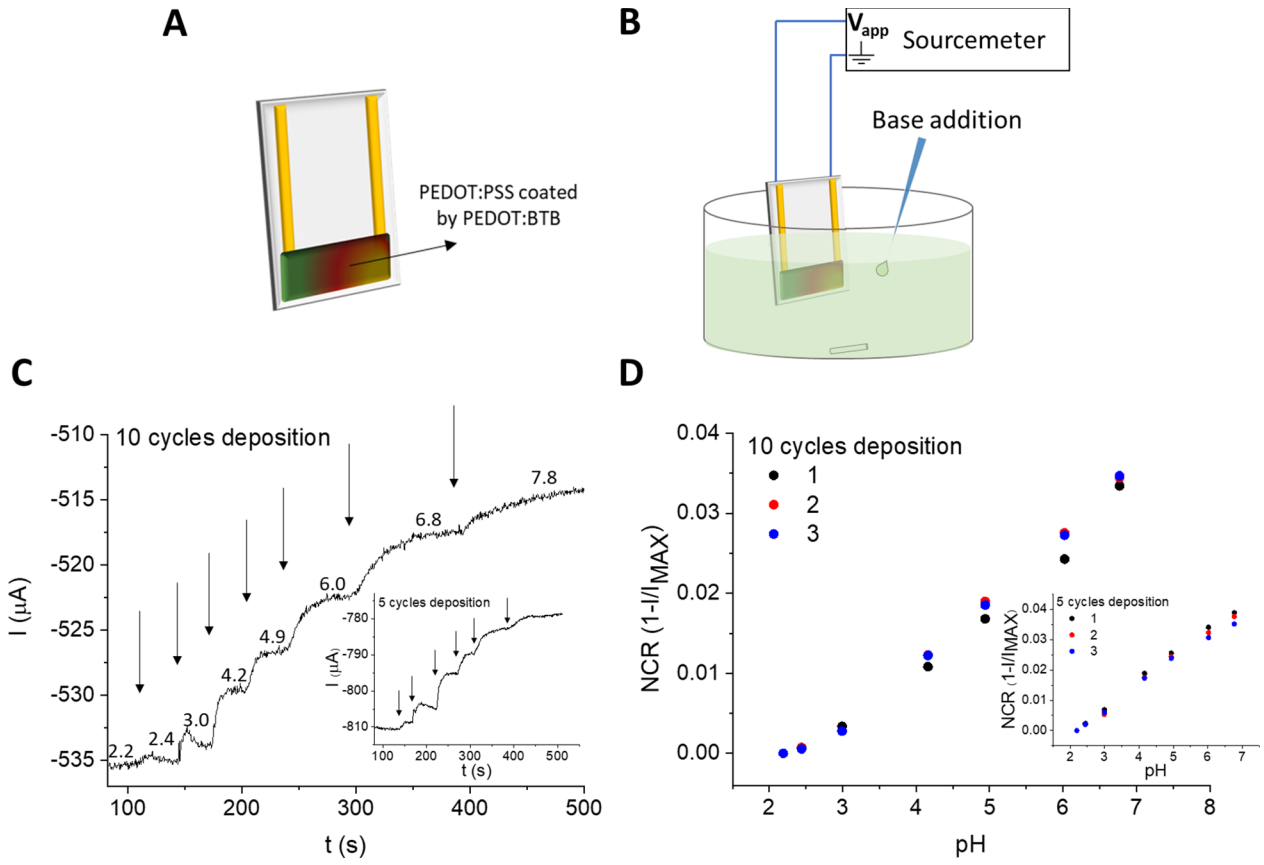

Fig. 3. pH sensing with the two-terminal device. Schematic illustrations of (A) the two-terminal sensor and (B) the experimental setup used for pH sensing. (C) Current vs. time response to pH variations in U.B. following base additions recorded with a sensor obtained by 10 cycles of deposition of PEDOT:BTB. $V_{app} = -200$ mV. Inset: response of a sensor obtained after 5 deposition cycles. (D) Normalized current response vs. pH recorded in three independent measurements with the device used in (C). Inset: repeatability of the sensor obtained using 5 deposition cycles.

without using a reference electrode. In the present work, we hypothesise that the pH-susceptible electromotive force generated at the PEDOT:BTB/electrolyte interface could exert a spontaneous electrochemical gating on a semiconducting channel, as long as the two materials were kept in electrical contact, thus resulting in a two-terminal pH sensor comprising a simple, single-channel device. The major advantage of this approach is the possibility of removing the gate electrode, with substantial simplification of the device architecture, which is comparable

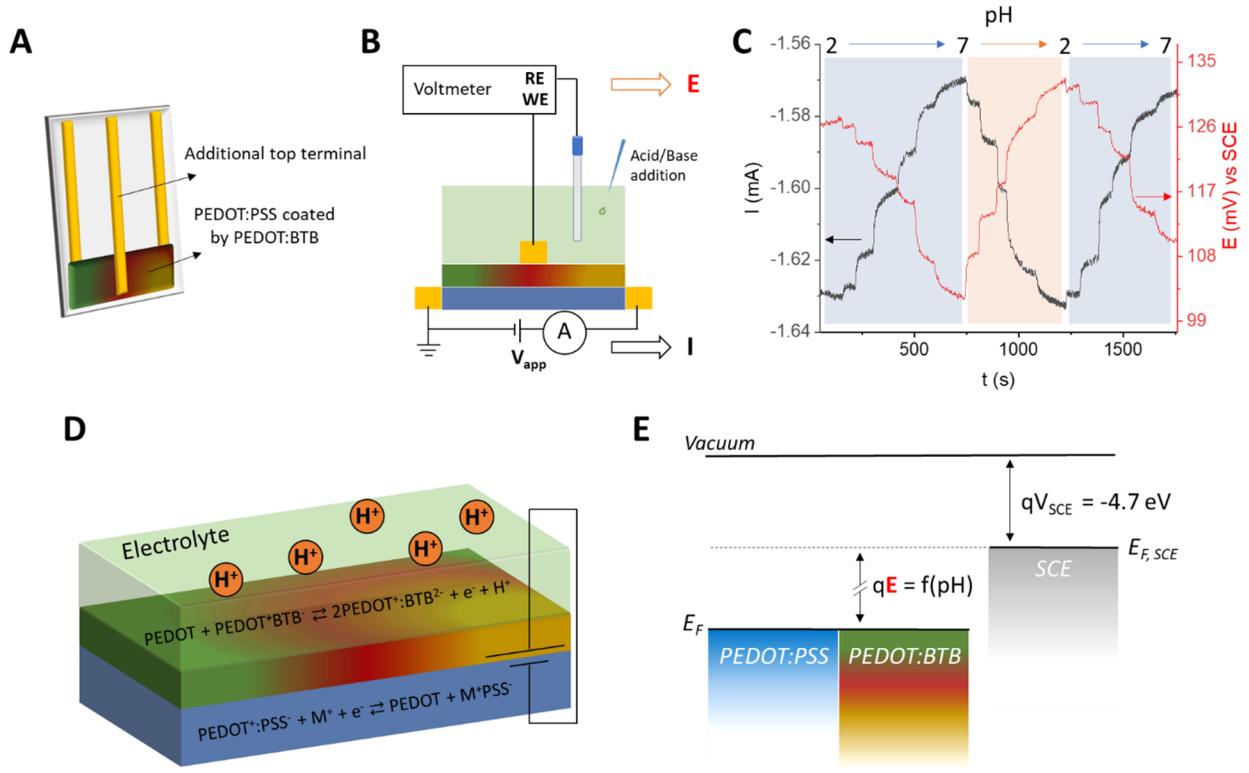

Fig. 4. Electrochemical gating in the pH sensor. Schematic illustrations of (A) the sensor with an additional gold track making contact with the sensing layer and (B) the experimental setup used to study the sensing mechanism. (C) Simultaneous recording of electrochemical potential and current upon variations in the pH of the electrolyte solution. $V_{app} = -200$ mV. (D) Schematic illustration of the proposed sensing mechanism. (E) Qualitative energy diagram illustrating the Fermi level shift due to pH variations. E_F = Fermi level of PEDOT in the polymeric films; $E_{F,SCE}$ = Fermi level of the reference electrode; q = electron charge; qV_{SCE} = reference electrode energy level; E = potential difference measured between the reference electrode and the PEDOT:BTB layer, which is a function of the electrolyte pH.

to that of a chemiresistor.

In order to fabricate the two-terminal pH sensor, PEDOT:BTB was electrochemically deposited directly on top of a PEDOT:PSS film connecting two gold tracks (Fig. S1A). After the functionalization, the composite material exhibits pH-dependent redox systems (Fig. S1B and C), while the presence of the new polymer layer slightly affects the electrical conductivity, which can be ascribed to the PEDOT:PSS (Table S1). Fig. 2 shows AFM characterisation of the morphology of the PEDOT:PSS and PEDOT:BTB/PEDOT:PSS layers.

A flattened surface is observed in the PEDOT:PSS layer, in accordance with literature data for spin-coated films [37], with a Root Mean Square (RMS) roughness of (0.6 ± 0.1) nm and a thickness of (610 ± 90) nm. Following electrodeposition, the morphology of the resulting PEDOT:BTB/PEDOT:PSS film is characterised by homogeneously distributed, discrete globular structures, similarly to those reported for electrochemically deposited PEDOT films [38,39]. The final RMS roughness and thickness were (2.8 ± 0.1) nm and (1.13 ± 0.07) × 10^3 nm, respectively.

A schematic illustration of the two-terminal device is given in Fig. 3A. For pH sensing, one terminal was connected to the ground, while a current I flowing through the PEDOT-based layers was generated upon application of a constant potential (V_{app}, optimized to −200 mV, based on the best sensing performances as reported in Table S2) to the second terminal (Fig. 3B).

Fig. 3C reports the response of a two-terminal sensor obtained after 10 cycles of PEDOT:BTB deposition. A similar response is recorded with a sensor obtained using 5 deposition cycles (inset to Fig. 3C). Upon base additions, I decreases stepwise until a steady-state value is reached. According to the performance observed in the potentiometric experiment (Fig. 1), a linear response is obtained in the pH range 2–7. At alkaline pH values, current drift is observed. Fig. 3D shows the repeatability of the sensor in terms of normalised current response (NCR) vs pH. The average NCR sensitivity was equal to (8.3 ± 0.2) × 10^{-3} pH unit^{-1} (N = 3, R^2 = 0.991) in the case of 5 deposition cycles and (7.5 ± 0.2) × 10^{-3} pH unit^{-1} (N = 3, R^2 = 0.987) for 10 deposition cycles, which can be expressed in terms of potential as 62 mV pH unit^{-1} and 56 mV pH unit^{-1}, respectively, based on our previous findings [32]. Therefore, this simple two-terminal device can be used as a two-point probe pH sensor, with important advantages compared to conventional technologies. Indeed, on the one hand, the performance of a potentiometric system is matched without the need to use a bulky reference electrode or ion-selective membranes. On the other hand, the three-terminal configuration, typical of organic transistor sensors, is simplified as the application of a second (gate) voltage, as well as the presence of a physical gate electrode, are no longer necessary.

3.3. Electrochemical gating in the two-terminal device

Although the major advantage of the electrochemical sensor investigated here is its simplified geometry, in that the application of a second voltage from an external source is not required, a three-terminal configuration was used to study the mechanism originating the sensor response. Therefore, a third gold track was evaporated between the two terminals of the device, on top of the sensing film, in order to connect the PEDOT:BTB layer with the read-out electronics (Fig. 4A).

The goal of this experiment was the simultaneous measurement of the electrochemical potential of the pH-sensing film (PEDOT:BTB) and the current variations occurring in the charge transport layer (PEDOT:PSS) during pH changes in the electrolyte solution. Therefore, the sensor was connected to a sourcemeter unit to apply a fixed voltage across the polymer layer and record the generated I. Concurrently, the

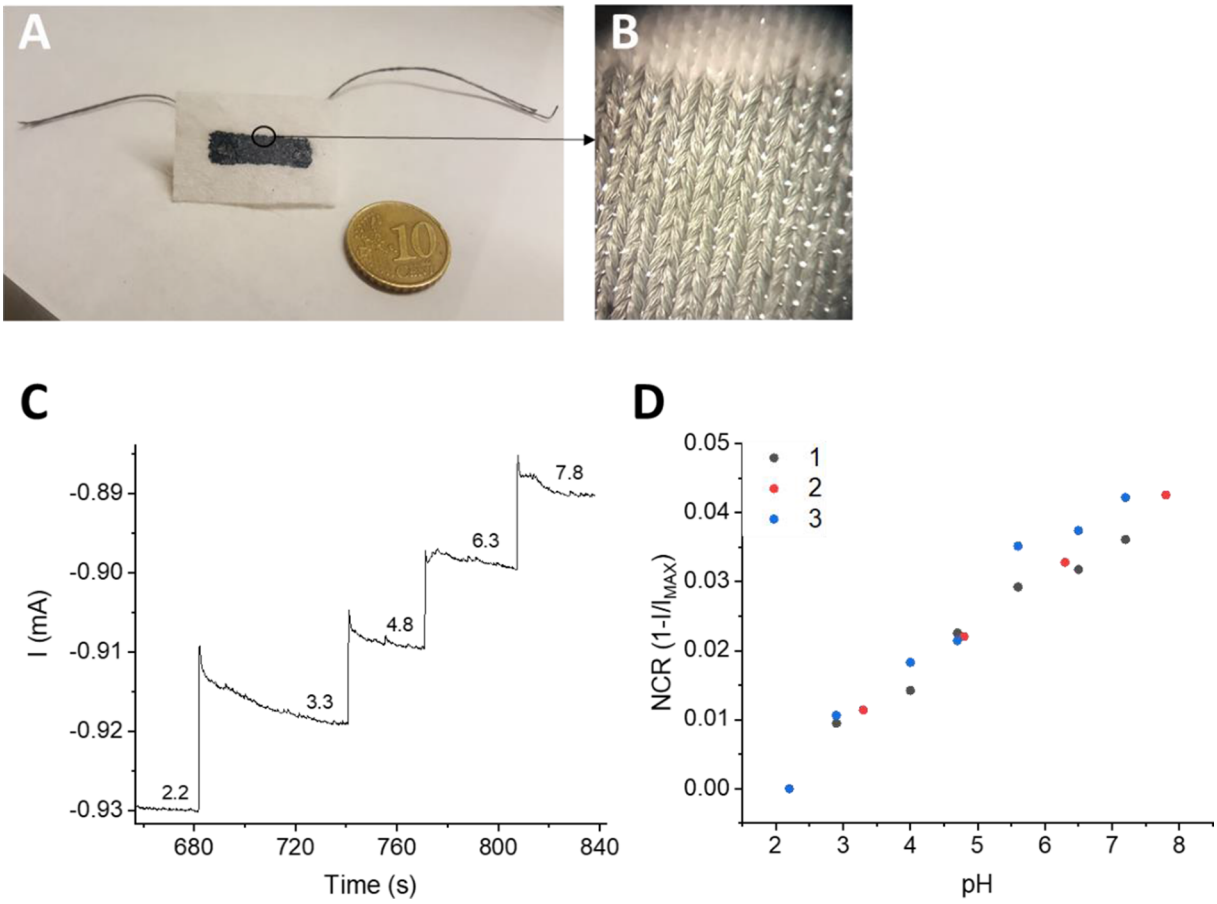

Fig. 5. Wearable two-terminal pH sensor. (A) Photo of the two-terminal wearable sensor and (B) magnification of the fabric knotwork. (C) Current vs time response to pH variations in U.B. following base additions obtained with the textile sensor. $V_{app} = -200$ mV. (D) Normalized current response vs pH recorded in three independent measurements with the device used in (C).

third terminal was employed as an indicator electrode to measure the electrochemical potential generated by the top layer with respect to a reference electrode (Fig. 4B). The two complementary sets of data (i.e., *E* and *I*) are plotted vs time upon reversible change of the electrolyte pH in Fig. 4C. In accordance with the potentiometric response observed in Fig. 1, the recorded *E* value decreases as the pH of the electrolyte increases. Note that the sub-Nernstian variations observed in this case are probably due to the presence of the additional gold track, which excludes the covered portion of the polymer film from interactions with the electrolyte solution. At the same time, the current flowing through the bottom organic film diminishes, as observed during assessment of the sensor response (Fig. 3). We explain this mutual effect by considering the interface between the two organic layers (Fig. 4D). Since the pH sensing layer is in electrical contact with the carrier transport layer, the two elements reach an equilibrium state where they have the same electrochemical potential (i.e., their Fermi levels are aligned). A pH-dependent electrochemical potential described by the Nernst equation is generated at the PEDOT:BTB/electrolyte interface and can be measured vs a reference electrode, whose potential value is stable and defined with respect to vacuum level. Therefore, on varying the pH of the electrolyte solution, a potential difference arises at the PEDOT:BTB/PEDOT:PSS interface and acts like an electromotive force, thus shifting the Fermi energy levels of the PEDOT:PSS film to recover an equilibrium state at the interface between the organic films (Fig. 4E). Overall, a spontaneous, electrochemically driven gating is the dominant sensing mechanism, which is able to control the charge carrier concentration in the PEDOT:PSS layer with high reproducibility and leads to the pH-dependent current recorded as the output signal of the two-terminal sensor.

The device geometry in Fig. 4A is analogous to that proposed by Wrighton's group in the first papers concerning OECTs [40–42], where the gate electrode was in electrical contact with the transistor channel and allowed direct control of the channel conductivity by means of a potentiostat and a reference electrode. The additional gold track, which we used in this experiment as an indicator electrode, can indeed be connected to a potentiostat to apply a fixed electrochemical potential to the system, thus acting as a gate electrode that modulates the conductivity of the organic film in a transistor-like fashion. In this way, transfer characteristics can be recorded in the U.B. (Fig. S2A), highlighting the transistor behaviour described for similar OECT geometries [28,40–42]. We calculated the transconductance g_m, defined as $\frac{\partial I}{\partial E}$, in order to evaluate the current variations induced by an external source of potential. In this case, g_m was (1.96 ± 0.02) mS, which is similar to the value calculated from the modulation obtained in the two-terminal configuration (Fig. S2B), which is (2.23 ± 0.09) mS. These results demonstrate that the PEDOT:BTB layer can be seen as the source of a spontaneous electrochemical gating that is able to modulate the conductivity of the carrier transport layer in response to electrochemical reactions involving pH, in analogy with the gate element in an organic transistor. Moreover, it is important to stress the fundamental difference that distinguishes the electrochemically gated sensor from chemiresistive electrical sensors based on conducting polymers, such as polyaniline (PANi). In the latter, pH transduction relies on H^+ adsorption that triggers non-redox doping by acid-base reactions and induces swelling of the polymer film, thus leading to variations in resistance [17]. In contrast, the two-terminal sensor reported here benefits from the robustness of a potentiometric-like transduction.

3.4. Fabrication of a textile-based pH sensor

The extremely simple architecture of the two-terminal pH sensor should lead to advancements in sensor development targeting real-life applications. For example, to develop a wearable chemical sensing device capable of real-time pH monitoring, we fabricated a two-terminal sensor on a bio-ceramic fabric (Fig. 5), highlighting the versatility of our architecture.

Fig. 5A and B show a photo of the textile pH sensor and an enlarged image of the knitted structure. A conducting ink made of PEDOT:PSS was screen printed onto the cloth using a shadow mask in order to pattern the desired geometry. Afterwards, the PEDOT:PSS layer was functionalized with PEDOT:BTB by electrochemical deposition using 10 deposition cycles (Fig. S3), to ensure complete coverage of the fibres in the sensing area. The textile pH sensor was tested in U.B. during base additions, upon application of a fixed V_{app} (-200 mV). The response is shown in Fig. 5C, where the stepwise decrements in I are again correlated with the increasing electrolyte pH. The repeatability of the textile sensor was assessed during three independent measurements (Fig. 5D), with a NCR sensitivity of $(7.5 \pm 0.3) \times 10^{-3}$ pH unit^{-1} ($N = 3$, $R^2 = 0.994$), which is comparable to the sensing performance obtained on glass. It is worth noting that, despite the very simple device structure and the absence of a reference electrode, very high repeatability is obtained, even on a textile substrate.

4. Conclusion

The two-terminal pH sensor reported here shows remarkable potential for sensor miniaturisation and the development of portable and wearable electrochemical probes. First, the chemiresistor-like geometry based on flexible, all-polymeric materials is compatible with photolithography-free, high throughput and low-cost fabrication techniques, such as screen-printing, and adapts to conformable substrates. Second, the selective transduction, intrinsic to the pH-sensitive bilayer organic structure, allows label-free detection and eliminates the need for ion-selective membranes or additional fragile components, thus providing the platform with compactness and robustness. Finally, the functionality gained by spontaneous electrochemical gating requires only one sensing element and the application of only one voltage, thus considerably reducing the power consumption and favouring integration into clothes or other real-life objects.

CRediT authorship contribution statement

Federica Mariani: Investigation, Data curation, Formal analysis, Writing - original draft. **Isacco Gualandi:** Conceptualization, Methodology, Supervision, Writing - review & editing. **Domenica Tonelli:** Funding acquisition, Supervision, Writing - review & editing. **Francesco Decataldo:** Investigation, Writing - review & editing. **Luca Possanzini:** Investigation, Writing - review & editing. **Beatrice Fraboni:** Funding acquisition, Supervision, Writing - review & editing. **Erika Scavetta:** Project administration, Funding acquisition, Supervision, Writing - review & editing.

Declaration of Competing Interest

The authors declare that they have no known competing financial interests or personal relationships that could have appeared to influence the work reported in this paper.

Acknowledgements

This work was supported by the National Operation Program (PON) of the Ministry of Education, University and Research (Project PON-MIUR 2018 (Italy) ARS01_00996: “TEX-STYLE - Nuovi tessuti intelligenti e sostenibili multi-settoriali per design creativo e stile made-in-Italy).

References

[1] J.A. Kellum, Determinants of blood pH in health and disease, Crit. Care 4 (1) (2000) 6, https://doi.org/10.1186/cc644.
[2] T. Hickish, A.D. Farmery, Acid–base physiology: new concepts, Anaesth. Intensive Care Med. 19 (2018) 239–244, https://doi.org/10.1016/j.mpaic.2012.09.003.
[3] J. Moyer, D. Wilson, I. Finkelshtein, B. Wong, R. Potts, Correlation between sweat glucose and blood glucose in subjects with diabetes, Diabetes Technol. Ther. 14 (2012) 398–402, https://doi.org/10.1089/dia.2011.0262.
[4] D.B. Luckie, M.E. Krouse, Cystic fibrosis: does CFTR malfunction alter pH regulation? Genetic disorders, IntechOpen (2013) 319–344, https://doi.org/10.5772/52342.
[5] W. Dang, L. Manjakkal, W.T. Navaraj, L. Lorenzelli, V. Vinciguerra, R. Dahiya, Stretchable wireless system for sweat pH monitoring, Biosens. Bioelectron. 107 (2018) 192–202, https://doi.org/10.1016/j.bios.2018.02.025.
[6] M.J. Patterson, S.D.R. Galloway, M.A. Nimmo, Effect of induced metabolic alkalosis on sweat composition in men, Acta Physiol. Scand. 174 (2002) 41–46, https://doi.org/10.1046/j.1365-201x.2002.00927.x.
[7] Z. Sonner, E. Wilder, J. Heikenfeld, G. Kasting, F. Beyette, D. Swaile, F. Sherman, J. Joyce, J. Hagen, N. Kelley-Loughnane, R. Naik, The microfluidics of the eccrine sweat gland, including biomarker partitioning, transport, and biosensing implications, Biomicrofluidics 9 (3) (2015) 031301, https://doi.org/10.1063/1.4921039.
[8] N. Mehmood, A. Hariz, R. Fitridge, N.H. Voelcker, Applications of modern sensors and wireless technology in effective wound management, J. Biomed. Mater. Res. Part B 102 (4) (2014) 885–895, https://doi.org/10.1002/jbm.b.33063.
[9] M. Qin, H. Guo, Z. Dai, X. Yan, X. Ning, Advances in flexible and wearable pH sensors for wound healing monitoring, J. Semicond. 40 (2019) 111607, https://doi.org/10.1088/1674-4926/40/11/111607.
[10] J.R. Windmiller, J. Wang, Wearable electrochemical sensors and biosensors: a review, Electroanalysis 25 (2013) 29–46, https://doi.org/10.1002/elan.201200349.
[11] R. Byrne, D. Diamond, Chemo/bio-sensor networks, Nat. Mater. 5 (2006) 421–424, https://doi.org/10.1038/nmat1661.
[12] P. Spitzer, K.W. Pratt, The history and development of a rigorous metrological basis for pH measurements, J. Solid State Electrochem. 15 (2011) 69–76, https://doi.org/10.1007/s10008-010-1106-9.
[13] W. Vonau, U. Guth, pH monitoring: a review, J. Solid State Electrochem. 10 (2006) 746–752, https://doi.org/10.1007/s10008-006-0120-4.
[14] M. Yuqing, C. Jianrong, F. Keming, New technology for the detection of pH, J. Biochem. Biophys. Methods 63 (2005) 1–9, https://doi.org/10.1016/j.jbbm.2005.02.001.
[15] E. Kress-Rogers, Solid-state pH sensors for food applications, Trends Food Sci. Technol. 2 (1991) 320–324, https://doi.org/10.1016/0924-2244(91)90735-2.
[16] M. Cuartero, G.A. Crespo, All-solid-state potentiometric sensors: a new wave for in situ aquatic research, Curr. Opin. Electrochem. 10 (2018) 98–106, https://doi.org/10.1016/j.coelec.2018.04.004.
[17] D.M. Wilson, Chemical sensors for portable, handheld field instruments, IEEE Sens. J. 1 (4) (2001) 256–274, https://doi.org/10.1109/7361.983465.
[18] J. Bobacka, A. Ivaska, A. Lewenstam, Potentiometric ion sensors, Chem. Rev. 108 (2008) 329–351, https://doi.org/10.1021/cr068100w.
[19] M. Kaisti, Detection principles of biological and chemical FET sensors, Biosens. Bioelectron. 98 (2017) 437–448, https://doi.org/10.1016/j.bios.2017.07.010.
[20] J. Janata, Potentiometric microsensors, Chem. Rev. 90 (1990) 691–703, https://doi.org/10.1021/cr00103a001.
[21] M. Sophocleous, J.K. Atkinson, A review of screen-printed silver/silver chloride (Ag/AgCl) reference electrodes potentially suitable for environmental potentiometric sensors, Sens. Actuat. A Phys. 267 (2017) 106–120, https://doi.org/10.1016/j.sna.2017.10.013.
[22] X. Ke, Micro-fabricated electrochemical chloride ion sensors: from the present to the future, Talanta 211 (2020) 120734, https://doi.org/10.1016/j.talanta.2020.120734.
[23] P. Bergeveld, Development of an ion-sensitive solid-state device for neurophysiological measurements, IEEE Trans. Bio. Med. Eng. BME 17 (1) (1970) 70–71, https://doi.org/10.1109/TBME.1970.4502688.
[24] Rosemount™ TF396 Non-Glass ISFET pH Sensor. https://www.emerson.com/en-us/catalog/rosemount-sku-tf396-non-glass-isfet-ph-sensor.
[25] Pocket ISFET pH Meter, Model 24006. https://www.deltatrak.com/isfet-ph-meters.
[26] CS526-L Digital ISFET pH Sensor. https://www.campbellsci.com/cs526.
[27] P. Bergeveld, Thirty years of ISFETOLOGY. What happened in the past 30 years and what may happen in the next 30 years, Sens. Actuat. B Chem. 88 (2003) 1–20, https://doi.org/10.1016/S0925-4005(02)00301-5.
[28] I. Gualandi, M. Tessarolo, F. Mariani, D. Tonelli, B. Fraboni, E. Scavetta, Organic electrochemical transistors as versatile analytical potentiometric sensors, Front. Bioeng. Biotechnol. 7 (2019) 354, https://doi.org/10.3389/fbioe.2019.00354.
[29] A. Spanu, F. Viola, S. Lai, P. Cosseddu, P.C. Ricci, A. Bonfiglio, A reference-less pH sensor based on an organic field effect transistor with tunable sensitivity, Org. Electron. 48 (2017) 188–193, https://doi.org/10.1016/j.orgel.2017.06.010.
[30] A. Caboni, E. Orgiu, E. Scavetta, M. Barbaro, A. Bonfiglio, Organic-based sensor for chemical detection in aqueous solution, Appl. Phys. Lett. 95 (12) (2009) 123304, https://doi.org/10.1063/1.3232252.
[31] G. Scheiblin, R. Coppard, R.M. Owens, P. Mailley, G.G. Malliaras, Referenceless pH sensor using organic electrochemical transistors, Adv. Mater. Technol. 1600141

(2017) 1–5, https://doi.org/10.1002/admt.201600141.
[32] F. Mariani, I. Gualandi, M. Tessarolo, B. Fraboni, E. Scavetta, PEDOT: dye-based, flexible organic electrochemical transistor for highly sensitive pH monitoring, ACS Appl. Mater. Interfaces 10 (2018) 22474–22484, https://doi.org/10.1021/acsami.8b04970.
[33] A. Mohtasebi, P. Kruse, Chemical sensors based on surface charge transfer, Phys. Sci. Rev. 3 (2) (2018) 20170133, https://doi.org/10.1515/psr-2017-0133.
[34] A.L. Ng, C.-F. Chen, H. Kwon, Z. Peng, C.S. Lee, Y.H. Wang, Chemical gating of a synthetic tube-in-a-tube semiconductor, J. Am. Chem. Soc. 139 (2017) 3045–3051, https://doi.org/10.1021/jacs.6b12111.
[35] I. Gualandi, M. Tessarolo, F. Mariani, T. Cramer, D. Tonelli, E. Scavetta, B. Fraboni, Nanoparticle gated semiconducting polymer for a new generation of electrochemical sensors, Sens. Actuat. B Chem. 273 (2018) 834–841, https://doi.org/10.1016/j.snb.2018.06.109.
[36] A. Balamurugan, Z.-W. Chen, S.-M. Chen, Electrochemical preparation of bromo thymol blue-PEDOT composite electrode and characterization, J. Electrochem. Soc. 155 (2008) E151, https://doi.org/10.1149/1.2969944.
[37] M. Marzocchi, I. Gualandi, M. Calienni, I. Zironi, E. Scavetta, G. Castellani, B. Fraboni, Physical and electrochemical properties of PEDOT:PSS as a tool for controlling cell growth, ACS Appl. Mater. Interfaces 7 (2015) 17993–18003, https://doi.org/10.1021/acsami.5b04768.
[38] V. Castagnola, C. Bayon, E. Descamps, C. Bergaud, Morphology and conductivity of PEDOT layers produced by different electrochemical routes, Synth. Met. 189 (2014) 7–16, https://doi.org/10.1016/j.synthmet.2013.12.013.
[39] Y. Vlamidis, M. Lanzi, E. Salatelli, I. Gualandi, B. Fraboni, L. Setti, D. Tonelli, Electrodeposition of PEDOT perchlorate as an alternative route to PEDOT:PSS for the development of bulk heterojunction solar cells, J. Solid State Electrochem. 19 (2015) 1685–1693, https://doi.org/10.1007/s10008-015-2802-2.
[40] H.S. White, G.P. Kittlesen, M.S. Wrighton, Chemical derivatization of an array of three gold microelectrodes with polypyrrole: fabrication of a molecule-based transistor, J. Am. Chem. Soc. 106 (1984) 5375–5377, https://doi.org/10.1021/ja00330a070.
[41] G.P. Kittlesen, H.S. White, M.S. Wrighton, Chemical derivatization of microelectrode arrays by oxidation of pyrrole and N-methylpyrrole: fabrication of molecule-based electronic devices, J. Am. Chem. Soc. 106 (1984) 7389–7396, https://doi.org/10.1021/ja00336a016.
[42] E.W. Paul, A.J. Ricco, M.S. Wrighton, Resistance of polyaniline films as a function of electrochemical potential and the fabrication of polyaniline-based microelectronic devices, J. Phys. Chem. 89 (1985) 1441–1447, https://doi.org/10.1021/j100254a028.